



Statistical analysis and Neural Network Modeling of functionally graded porous nanobeams vibration in an elastic medium by considering the surface effects

Xiaofei Cheng^{a,*}, Sara Hakem Al-Khafaji^b, Mohammad Hashemian^{c,*}, Mariem Ahmed^d, S. Ali Eftekhari^{c,*}, Ali Ihsan Alanssari^e, Nabaa Muhammad diaa^f, Manal Morad Karim^g, Davood Toghraie^{c,*}, Ahmed Hussien Alawadi^h

^a Qingdao Huanghai University, Qingdao, Shandong, 266427, China

^b Department of Media, Al-Mustaqbal University College, Babylon, 51001, Iraq

^c Department of Mechanical Engineering, Khomeinishahr Branch, Islamic Azad University, Khomeinishahr, Iran

^d College of pharmacy, Al-Farahidi university, Iraq

^e Department of Medical Laboratories Technology, Al-Nisour University College, Iraq

^f Department of Construction Engineering & Project Management, AlNoor University, College, Nineveh, Iraq

^g National University of Science and Technology, Dhi Qar, Iraq

^h College of technical engineering, The islamic University, Najaf, Iraq

ARTICLE INFO

Keywords:

Statistical analysis
Neural network modeling
Functionally graded porous nanobeams
Elastic medium
Surface effects

ABSTRACT

The natural frequency of a clamped–clamped functionally graded porous (FGP) nanobeam is predicted in this study. Material distribution is considered based on monotonous, symmetric, and non-symmetric patterns in the thickness direction. This paper deals with governing equations of nanobeams based on third-order shear deformation beam theory in conjunction with nonlocal strain gradient theory (NSGT) and surface effects. Artificial neural network (ANN) is utilized to predict the effect of eight parameters including temperature gradient, residual surface stress, porosity distribution pattern, porosity parameter, nonlocal and material length scale parameters, and elastic and shear coefficients of Pasternak foundation on the fundamental frequency of FGP nanobeam. Different training methods are selected to simulate input and output dependency. Results show that the dependency of the natural frequency is inverse to the temperature gradient and nonlocal parameter in the sense that increasing these factors will decrease the natural frequency. Also, increasing the material length scale parameter grows the effect of the nonlocal parameter. Residual surface stress, material length scale, and Pasternak foundation parameters have a direct effect on the output and among them; the material length scale parameter has a more noticeable effect. Finally, it was found that by increasing the porosity parameter value, the diversity of natural frequency levels up drastically

1. Introduction

In nature, many materials including wood, sponge, bone, etc., are in the category of porous materials. Utilizing porous materials is a common solution for reducing the weight of structures. This category of materials has a very low density due to the presence of small pores inside them. Pores usually were embedded in a solid matrix. In addition to low density, porous materials are good sound insulators, and have a significant energy absorption capacity. Furthermore, they are highly recyclable and exhibit low thermal and electrical conductivity. It is noteworthy that despite mentioned features, porous materials have lower stiffness and fracture strength in comparison to homogeneous

ones. Thus, to fix this problem, sandwich structures and functionally graded porous materials (FGPMs) were utilized (Chen et al., 2016; Xiang et al., 2017; Foroutan et al., 2021). Bending and buckling analyses of functionally graded porous (FGP) beams were reported by Chen et al. (2015). Elastic modulus and density change in the thickness direction of the Timoshenko beam considering both symmetric and non-symmetric porosity distribution patterns. Ritz method was utilized to evaluate the critical buckling load and maximum deflection of the beam. A novel method was introduced for free vibration and bending analyses of FGP plates by Yin et al. (2021). Results show under the same values of porosity parameter; maximum deflection occurs in the even-distributed porous plate in contrast to uneven one. Gong et al. (2019) developed a

* Corresponding authors.

E-mail addresses: chengxiaofei2023@163.com (X. Cheng), Hashemian@iaukhsh.ac.ir (M. Hashemian), a.eftekhari@iaukhsh.ac.ir (S.A. Eftekhari), Toghraee@iaukhsh.ac.ir (D. Toghraie).

<https://doi.org/10.1016/j.engappai.2023.106313>

Received 5 July 2022; Received in revised form 3 February 2023; Accepted 8 April 2023

Available online xxxx

0952-1976/© 2023 Elsevier Ltd. All rights reserved.

nonlinear thermoelastic analysis of FGPMs considering the cell-vertex finite volume method. Based on the results, unlike thermal stress, deformation and temperature were influenced by porosity distribution patterns poorly. She et al. (2018) performed nonlinear bending and vibration of FGP tubes using a novel tube framework and NSGT. On this basis, Even and uneven porosity distributions were assumed in functionally graded metal–ceramic tubes.

The most important difference between elasticity fundamental equations of classical (macro) and non-classical (micro and nano) structures is related to constitutive equations. Unlike classical continuum mechanics, in non-classical one, size effect has appeared in the stress–strain relation of the material considering the stress of each point is not only the function of mentioned point strain. Modified couple stress (MCS), nonlocal elastic stress (Eringen), strain gradient (SG), modified strain gradient (MSG), second strain gradient, and nonlocal strain gradient theories can be numbered as non-classical ones. Mindlin (1965) utilized strain and its first and second gradient in potential energy density of elastic solid materials as second strain gradient theory. Based on Eringen's theory, stress at any point of the body is a function of the strain at all points of the body (Eringen, 1983). Fleck and Hutchinson (2001) ignoring higher-order equilibrium equations, proposed the SG theory. Stretch gradient and rotation gradient tensors as the components of deformation gradient tensor were introduced in SG theory. The equilibrium of moments of couples was considered by Yang et al. (2002) in MCS theory. MSG as a three-parameter length scale theory proposed by Lam et al. (2003) disregarding the effect of anti-symmetric component of rotation gradient tensor in strain energy. Lim et al. (2015) extended Eringen theory by introducing new kernel function in internal energy density potential. Higher order strain gradient term in addition to nonlocal stress was utilized in this theory namely NSGT. Utilizing nonlocal theory, forced vibration of porous nanobeams in hygro-thermal environment was conducted by Barati (2017). On this basis, nonlocal theory predicts lower resonance frequencies for an FGP beam in comparison to a local one. Based on FEM a ten-degree beam element proposed for nonlocal thermo-elastic analysis of FGP nanobeams by Aria et al. (2019). Li et al. (2018) developed implementation of NSGT in nanobeams considering thickness effect. According to this study neglecting strain gradient in thickness direction leads to misleading in strain energy calculation. Contribution of thickness effect in bending of porous nanobeams was reported by Tang et al. (2019a). Considering thickness effect and NSGT vibration analysis of nanobeams (Tang et al., 2019b), nonlinear dynamic stability of nanobeams (Chen et al., 2019b), and nonlinear free vibration of nanobeams (Chen et al., 2019a) have been focused in the literature.

Due to the high surface to volume ratio of nanostructures, the effects of surface tension play a very important role in the mechanical behavior of this type of structures (Eltaher et al., 2013; Lu et al., 2019; Rafeian et al., 2017). On the micro and nano scales, the surface atoms of the material are in different equilibrium conditions than the bulk atoms, which originates from the difference in the energies of the two mentioned parts. Therefore, in nano dimensions, the material surface is considered as a layer with different mechanical and energy properties. Therefore, the surface of the nanostructure can be considered as a layer with a certain energy and connected to the bulk. Gurtin and Murdoch by adding surface tension effects, presented the theory of non-classical elasticity of surface tension effects (Gurtin and Murdoch, 1975; Gurtin and Ian Murdoch, 1978). Bending, buckling and vibration of FGP nanobeams developed by Enayat et al. (2020a,b) based on NSGT and Gurtin–Murdoch surface theory. The effect of different parameters such as porosity distribution pattern, nonlocal parameter, material length scale parameter and surface characteristic on the critical buckling load and fundamental frequency were discussed in this study. Babaei and Eslami (2021) reported nonlinear vibration and snap-through buckling of FGP panels considering NSGT. Uniform porosity distribution pattern implemented in radial direction. They showed increasing the porosity coefficient results in an increase in the nonlinear to linear frequency

ratio ANN approach was used by researchers to predict the behavior of different systems (Ahmad, 2022; Chen, 2022; Deng et al., 2022; Hanif et al., 2022; Khan et al., 2022; Sharma et al., 2022).

Kao and Hung (2003) examined damage detection in structures using vibration analysis. ANN approach was employed to identify the system state in the first step and to generate free vibration response in the next step. Garg et al. (2022) implemented Gaussian process regression (GPR) to compare stiffness prediction based on final stiffness matrix and superposition of sub-matrices. ANN model in conjunction with uncertainty quantification algorithm was used to determine stochastic natural frequency in composite plates by Dey et al. (2016). Stochastic buckling of sandwich plates regarding zigzag theory was presented by Kumar et al. (2019). Truong et al. (2020) optimized material distribution in bidirectional functionally graded beams with the aid of ANN-differential evolution method. Finally, non-uniform rational b-spline functions were suggested as optimal material distribution. Al Rjoub and Alshatnawi (2020) utilized ANN technique to predict natural frequency of FGP plate based on third-order shear deformation theory. free vibration of functionally graded beams was estimated considering ANN approach by Yildirim (2021). The effects of different inputs such as grading direction, slenderness ratio, material properties, and grading index on the first five natural frequencies were studied in this research. Maurya et al. (2021) investigated delamination in carbon fiber reinforced polymer matrix using ANN and FEM. ANN was utilized to predict the length and location of delamination based on the first three natural frequencies in this survey.

According to the authors' knowledge, the ANN approach was not implemented to predict the natural frequency of FGP nanobeams based on NSGT and surface effects. Nanobeam is rested on Pasternak foundation and different porosity distribution patterns are considered in the thickness direction. Finally, the detailed parametric study investigates the effect of nonlocal and material length scale parameters, temperature gradient, porosity distribution, porosity parameter, surface residual stress, and foundation parameters on the natural frequency variation of the FGP nanobeam.

2. Governing equations

2.1. Problem schematic

An FGP nanobeam with a rectangular cross-section is presented in Fig. 1. Length, width and height of the nanobeam are presented by L , b and h , respectively. The nanobeam is rested on the Pasternak Foundation as a two-variable elastic medium with elastic and shear stiffness coefficients k_w and k_G , respectively. x and z are the axes of the Cartesian coordinate indicating axial and transverse directions of the nanobeam. Also; u and w denote corresponding displacements along mentioned axes. Utilizing Reddy beam theory, cross-section rotation (φ) is considered in this survey.

Porosity distribution changes in nanobeam as a function of Z in transverse direction. Monotonous, symmetric and non-symmetric distribution patterns are utilized in this research. As shown in Fig. 2, in monotonous type the distribution of porosities is uniform along Z -direction. In symmetric one, the porosity has the higher density near the middle surface of the beam and finally, in the non-symmetric pattern the density of the pores becomes less along Z -direction. Mechanical properties of the FGP beam ($P(z)$); containing bulk Young's modulus (E), bulk density (ρ), thermal coefficient parameter (α), and residual surface stress (τ_0^s) can be considered as,

$$P(z) = P_0 (1 - e_1 f(z)), \quad (1)$$

in which $0 \leq e_1 < 1$ is porosity parameter and P_0 indicates mentioned parameters as porosity effect is neglected. In addition:

$$f(z) = \begin{cases} \eta = \frac{1}{e_1} \left\{ 1 - \left[\frac{2}{\pi} \left(\sqrt{1 - e_1} - 1 \right) + 1 \right]^2 \right\}, & \text{for Monotonous} \\ \cos\left(\frac{\pi z}{h}\right), & \text{for Symmetric} \\ \cos\left(\frac{\pi z}{2h} + \frac{\pi}{4}\right). & \text{for Non-symmetric} \end{cases} \quad (2)$$

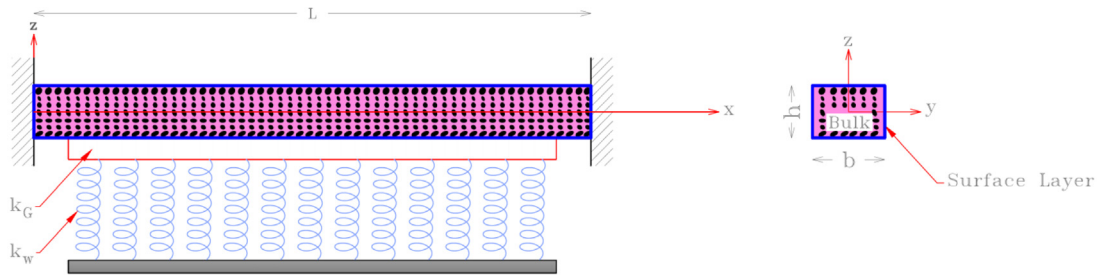


Fig. 1. Schematic of the FGP nanobeam rested on Pasternak foundation.

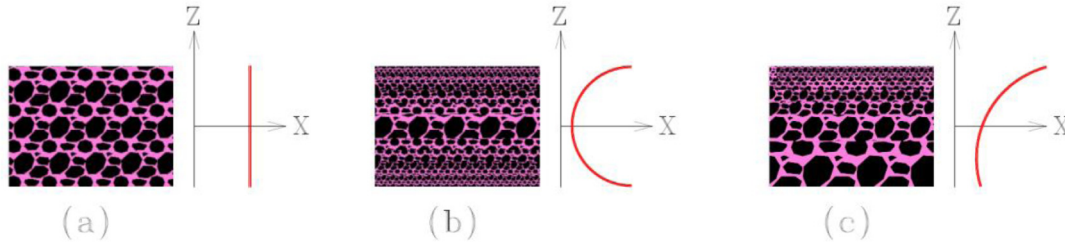


Fig. 2. Porosity distribution pattern: (a) Monotonous, (b) Symmetric, (c) Non-symmetric.

In contrast to above mentioned mechanical parameters, the density parameter (ρ) of the FGP beam has a different variation along thickness direction:

$$\text{Monotonous : } \rho(z) = \rho_0 \sqrt{1 - e_1 \eta},$$

$$\text{Symmetric : } \rho(z) = \rho_0 \left[1 - e_m \cos\left(\frac{\pi z}{h}\right) \right], \quad (3)$$

$$\text{Non - symmetric : } \rho(z) = \rho_0 \left[1 - e_m \cos\left(\frac{\pi z}{2h} + \frac{\pi}{4}\right) \right],$$

where

$$e_m = 1 - \sqrt{1 - e_1}. \quad (4)$$

2.2. Constitutive equations

According to surface elasticity theory, the outer layer of the nanobeam does not obey the constitutive equations of interior material (bulk). The surface layer is considered as a zero-thickness layer surrounding the bulk. There is no slippage between adjacent atoms of the surface layer and bulk. NSGT and Gurtin–Murdoch theories are considered as bulk and surface constitutive equations, respectively. Based on NSGT and EBT, the stress–strain relation of the bulk material can be stated as (Lim et al., 2015):

$$\left[1 - (e_1 a)^2 \nabla^2 \right] \left[1 - (e_0 a)^2 \nabla^2 \right] \sigma_{xx} = E \left[1 - (e_1 a)^2 \nabla^2 \right] \varepsilon_{xx} - E l^2 (1 - (e_0 a)^2 \nabla^2) \nabla^2 \varepsilon_{xx}, \quad (5)$$

where σ_{xx} indicates normal stress component and related strain component is depicted by ε_{xx} . e_0 and e_1 are the nonlocal material constants. The difference is that e_1 refers to first-order strain gradient field. l and a indicate material length scale parameter and internal characteristic length, respectively. According to Gurtin–Murdoch theory (Gurtin and Murdoch, 1975), the interaction of surface layer and bulk material impresses stress field in z direction. Counting mentioned interaction, thermal environment, $\nabla^2 = \frac{\partial^2}{\partial x^2}$ for EBT, $e_1 = e_0 = e$ and neglecting terms of order $O(\nabla^4)$ (Lim et al., 2015), stress field of bulk material can be rewritten as:

$$\left[1 - (ea)^2 \frac{\partial^2}{\partial x^2} \right] \sigma_{xx} = \left(1 - l^2 \frac{\partial^2}{\partial x^2} \right) \left[E (\varepsilon_{xx} - \alpha \Delta T) + \frac{2\nu z}{h} \left(\tau^s \frac{\partial^2 w}{\partial x^2} - \rho^s \frac{\partial^2 w}{\partial t^2} \right) \right], \quad (6)$$

$$\left[1 - (ea)^2 \frac{\partial^2}{\partial x^2} \right] \sigma_{xz} = \left(1 - l^2 \frac{\partial^2}{\partial x^2} \right) (G \gamma_{xz}),$$

where σ_{xz} and γ_{xz} are the shear stress and shear strain components, respectively. ν is poisson’s ratio, ΔT is thermal gradient, τ^s and ρ^s are residual surface stress and surface density. It is worth mentioning that superscript “s” is utilized to exhibit corresponding parameters of the surface layer. The combination of NSGT and Gurtin–Murdoch theory results in stress–strain relation of the surface layer as (Enayat et al., 2020a,b),

$$\left[1 - (ea)^2 \nabla^2 \right] \sigma_{xx}^s = (1 - l^2 \nabla^2) (E^s \varepsilon_{xx} + \tau^s),$$

$$\left[1 - (ea)^2 \nabla^2 \right] \sigma_{xz}^s = (1 - l^2 \nabla^2) \left[\tau^s \left(\frac{\partial w}{\partial x} \right) \right]. \quad (7)$$

The energy method in conjunction with Hamilton’s principle leads to final governing equations (Enayat et al., 2020a,b). Following discretized algebraic equations can be arranged after Employing GDQM as (Enayat et al., 2020b; Foroutan et al., 2020)

$$[M] \{\ddot{v}\} + [K] \{v\} = \{0\}, \quad (8)$$

where $[M]_{3N \times 3N}$ and $[K]_{3N \times 3N}$ are the mass and stiffness matrices, respectively and N is the number of grid points and

$$\{v\}_{3N \times 1} = \begin{Bmatrix} \{U\}_{N \times 1} \\ \{W\}_{N \times 1} \\ \{\varphi\}_{N \times 1} \end{Bmatrix}. \quad (9)$$

For the sake of simplicity and generality, dimensionless groups were defined in the components of the above matrices as (Enayat et al., 2020b)

$$\zeta = \frac{x}{L}, \quad U = \frac{u}{L}, \quad W = \frac{w}{L}, \quad \mu = \frac{ea}{L}, \quad \lambda = \frac{l}{L}, \quad \tau = \frac{t}{L} \sqrt{\frac{E_0}{\rho_0}},$$

$$K_W = \frac{k_w L^2}{A_0^*}, \quad K_G = \frac{k_G}{A_0^*}, \quad (10)$$

where

$$A_0^* = \int_{-h/2}^{h/2} E(z) dz + 2 \int_{-h/2}^{h/2} E^s(z) dz + b \left[E^s\left(\frac{h}{2}\right) + E^s\left(-\frac{h}{2}\right) \right]. \quad (11)$$

3. ANN configuration

ANN is a contraction of Artificial Neural Network and is known as one of the Artificial Intelligence (AI) tools widely used for different

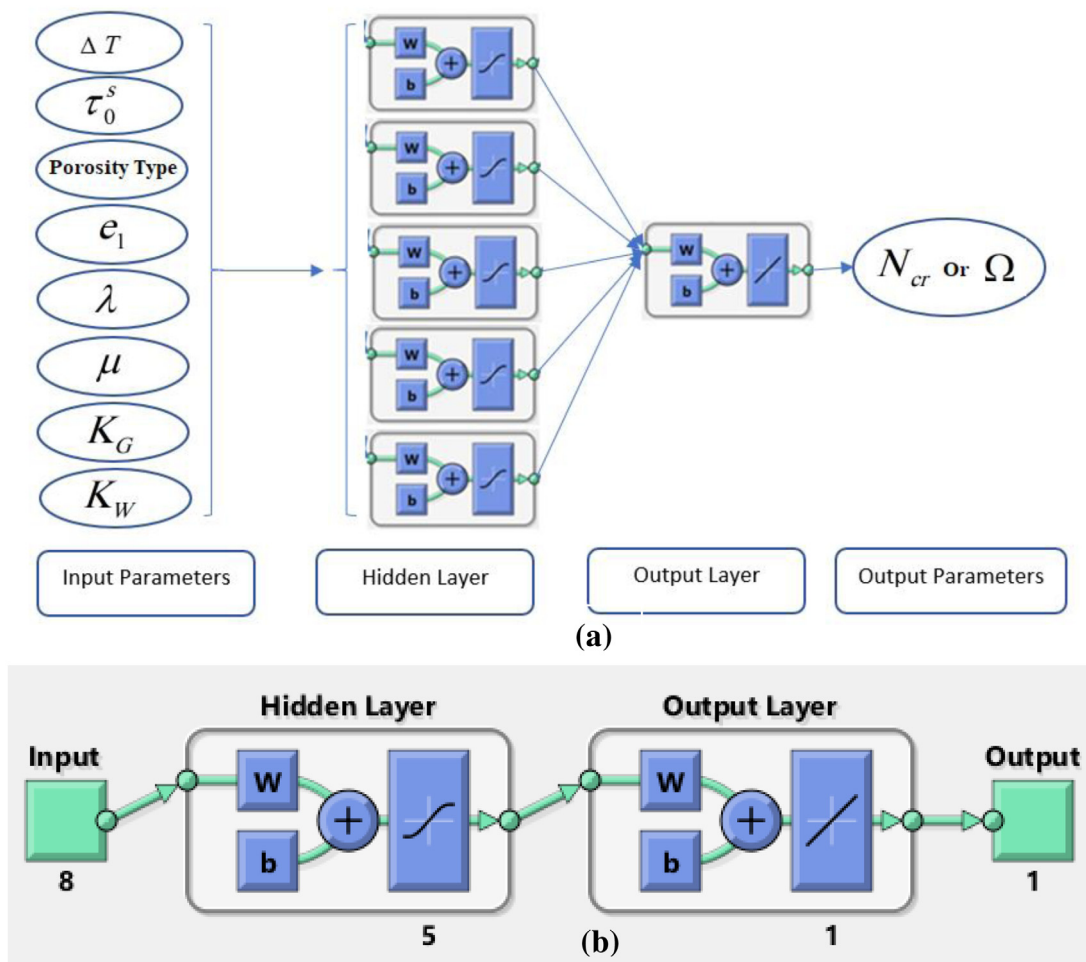


Fig. 3. (a) A multilayer perceptron ANN graph alongside inputs and outputs data, (b) ANN used in this study as a predictor.

objectives such as fitting function, classifying data and prediction of time series (Moshayedi et al., 2022; Naeimi et al., 2014; Xie et al., 2022). Also, in conjunction with an optimization method such as GA, SA, or PSO, an ANN shows high potential in determining the optimum state of the problem. This intelligent system handles data and it is originally inspired by the brain. Similar to the human brain, ANNs are consistent with many parallel processing units called neurons working alongside to solve a problem (Anon, 1995). For curve fitting applications, neural nets are usually configured of several successive layers each containing several neurons. These networks are categorized into different types according to data direction in the network. If the data stream is only from input to output direction, the network is called feedforward. On the other hand, some networks handle data in both directions, the latter is called recurrent network. The best type of curve fitting ANN is a multilayer feed-forward network (Hashemzadeh et al., 2017), therefore, in this manuscript, a two-layer Perceptron ANN is used for modeling the input–output relation of the natural frequency of an FGP nanobeam rested on an elastic medium considering surface effects versus different input parameters. This configuration is a simple and reliable topology for curve fitting used in many references showing its capabilities. This methodology is well developed and described in various Xia et al. (2022) and Fan et al. (2022). Eight parameters were investigated in this study including temperature gradient, residual surface stress, porosity distribution pattern, porosity parameter, nonlocal and material length scale parameters and elastic and shear coefficients of Pasternak foundation. The ANN is schematically depicted in Fig. 3(a). To simulate the input–output nonlinear dependency, usually Tangent Hyperbolic Sigmoid transfer functions (*tansig*) are used in the

second layer while the output layer has linear functions. Then, the ANN topology (including layer numbers, hidden layer neuron number and transfer function of each layer) is chosen by trial and error to obtain the lowest error/highest performance. Then, the ANN should be trained. According to that, various training methods are used and the best method is chosen for simulation of natural frequency functionality to input variables. Because ANN training has a random basis, the training of each method is repeated 50 times and the best condition is considered.

In Fig. 3(a), the 8 input parameters are presented alongside network-layer configuration as well as natural frequency as the sole output parameter. In Fig. 3(b), the schematic of the simulated network in MATLAB is depicted. The raw data for the training network is divided into 4 pairs of parameters and reported in Tables 1 to 4. 210 various samples were obtained from different combinations of these tables versus eight aforementioned input parameters and were used for the ANN training stage. Various criteria are implemented to assess the efficiency of trained ANN, for this reason, the total dataset is divided into three categories called “Learning Data (70%)”, “Validation Data (15%)” and “Test Data (15%)” to compare their error rate. It is worth mentioning that these categories are randomly selected by the training method.

In Table 5, the information about each parameter and its level is summarized.

In Fig. 4, the results of ANN training with 10 various learning methods are summarized and according to this figure and Table 6, the *trainbr* algorithm has the best performance. Hence, in the following

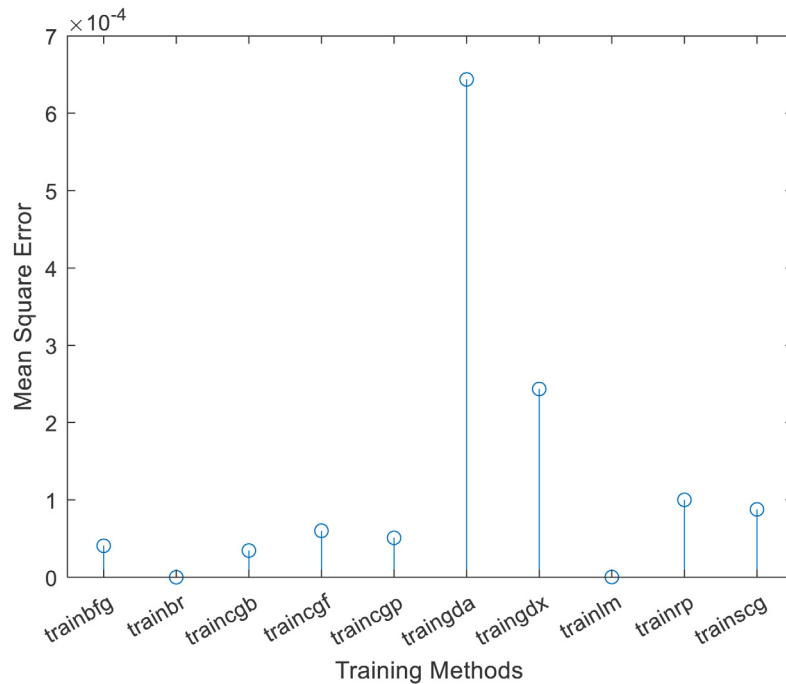


Fig. 4. Comparison of various training methods and their ANN performance.

Table 1

Natural frequency versus temperature gradient and residual surface stress for FGP nanobeam resting on an elastic foundation.

	$\Delta T (K)$	0	21.4	42.9	64.3	85.7	107.1	128.6	150	171.4	192.9	214.3	235.7	257.1	278.6	300
τ_0^s ($\frac{N}{m}$)	0.890	1.007	1.002	1.001	0.996	0.994	0.992	0.989	0.986	0.982	0.979	0.976	0.973	0.97	0.966	0.962
	0.000	0.89	0.887	0.883	0.88	0.876	0.873	0.869	0.866	0.862	0.859	0.856	0.852	0.848	0.843	0.839
	-0.890	0.754	0.749	0.745	0.742	0.737	0.732	0.728	0.723	0.719	0.714	0.71	0.706	0.701	0.698	0.692

Table 2

Natural frequency versus porosity parameter and porosity distribution pattern for FGP nanobeam resting on an elastic foundation.

e_1	0.000	0.060	0.130	0.190	0.260	0.320	0.390	0.450	0.510	0.580	0.640	0.710	0.770	0.840	0.900
Non-symmetric	1.020	1.010	1.000	0.993	0.984	0.975	0.963	0.953	0.940	0.926	0.911	0.893	0.873	0.849	0.821
Symmetric	1.020	1.020	1.020	1.020	1.020	1.020	1.030	1.030	1.030	1.040	1.040	1.050	1.050	1.070	1.090
Monotone	1.020	1.010	0.998	0.987	0.975	0.963	0.951	0.936	0.921	0.903	0.885	0.863	0.840	0.811	0.775

Table 3

Natural frequency versus nonlocal and material length scale parameters for FGP nanobeam resting on an elastic foundation.

μ	0	0.007	0.014	0.021	0.029	0.036	0.043	0.05	0.057	0.064	0.071	0.079	0.086	0.093	0.1
λ	0	0.719	0.720	0.719	0.719	0.719	0.718	0.718	0.718	0.717	0.717	0.716	0.715	0.715	0.714
	0.03	0.785	0.784	0.784	0.784	0.784	0.783	0.782	0.78	0.779	0.778	0.776	0.775	0.773	0.771
	0.06	0.880	0.879	0.880	0.878	0.877	0.876	0.875	0.872	0.87	0.868	0.865	0.862	0.859	0.856
	0.1	1.035	1.035	1.033	1.033	1.031	1.028	1.026	1.024	1.02	1.016	1.012	1.008	1.003	0.998

Table 4

Natural frequency versus elastic foundation parameters for FGP Nano-Beam resting on elastic foundation.

K_w	0	0.007	0.014	0.021	0.029	0.036	0.043	0.05	0.057	0.064	0.071	0.079	0.086	0.093	0.1
K_G	0.0001	0.992	0.996	0.999	1.003	1.005	1.008	1.011	1.014	1.017	1.019	1.023	1.025	1.029	1.034
	0.005	1.033	1.036	1.039	1.042	1.045	1.047	1.050	1.053	1.056	1.059	1.062	1.064	1.067	1.073
	0.01	1.073	1.076	1.078	1.081	1.084	1.087	1.089	1.092	1.095	1.098	1.100	1.103	1.106	1.109
	0.02	1.147	1.150	1.152	1.155	1.157	1.160	1.163	1.165	1.168	1.171	1.173	1.176	1.178	1.181

analysis, the ANN trained with this algorithm will be used for the prediction of natural frequency and more investigation.

To assess the ANN learning level, performance and correlation plots of the trained network are shown in Figs. 5 and 6.

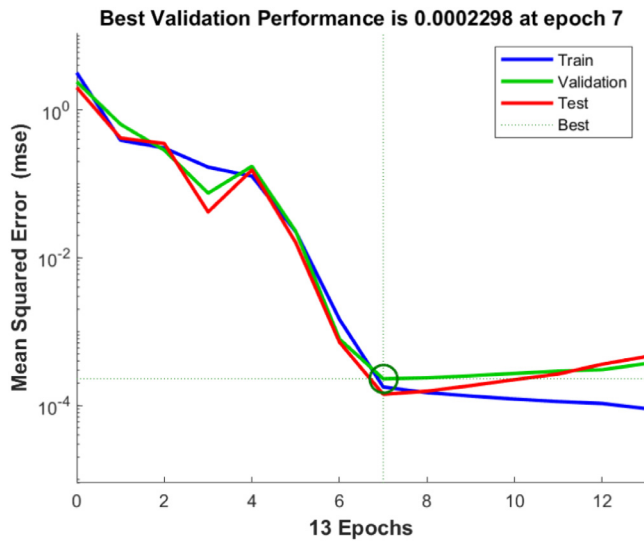


Fig. 5. Performance plot of trained network.

According to the above figures well training state of the network can be concluded, because firstly all of the data points are located on the bisector of the plane, secondly, the R-square value is 0.99992 which

Table 5

Parameters range and levels.

Parameter	Min	Max	No. of levels
$\Delta T (K)$	0	300	15
τ_0^*	-0.89	0.89	3
e_1	0	0.9	15
λ	0	0.1	4
μ	0	0.1	15
K_G	0.0001	0.02	4
K_W	0.01	0.1	15

is close to 1. Another plot for checking the ANN capability is shown in Fig. 7. In this plot, the true values are depicted using blue dots and the ANN outputs are plotted using red circles. There is a good match between these data.

As depicted in Figs. 8–11, ANN output is plotted alongside true values for natural frequency versus input parameter pairs. According to these figures, a very good match is observed between true data shown in blue dots and the surfaces attained from ANN, which proves the proper level of ANN training and the capability of this network to predict natural frequency considering every combination of input parameters.

For better understanding and analysis of parameters effects on the natural frequency and its deviation, Figs. 12 and 13 show output dependency on temperature gradient and residual surface stress.

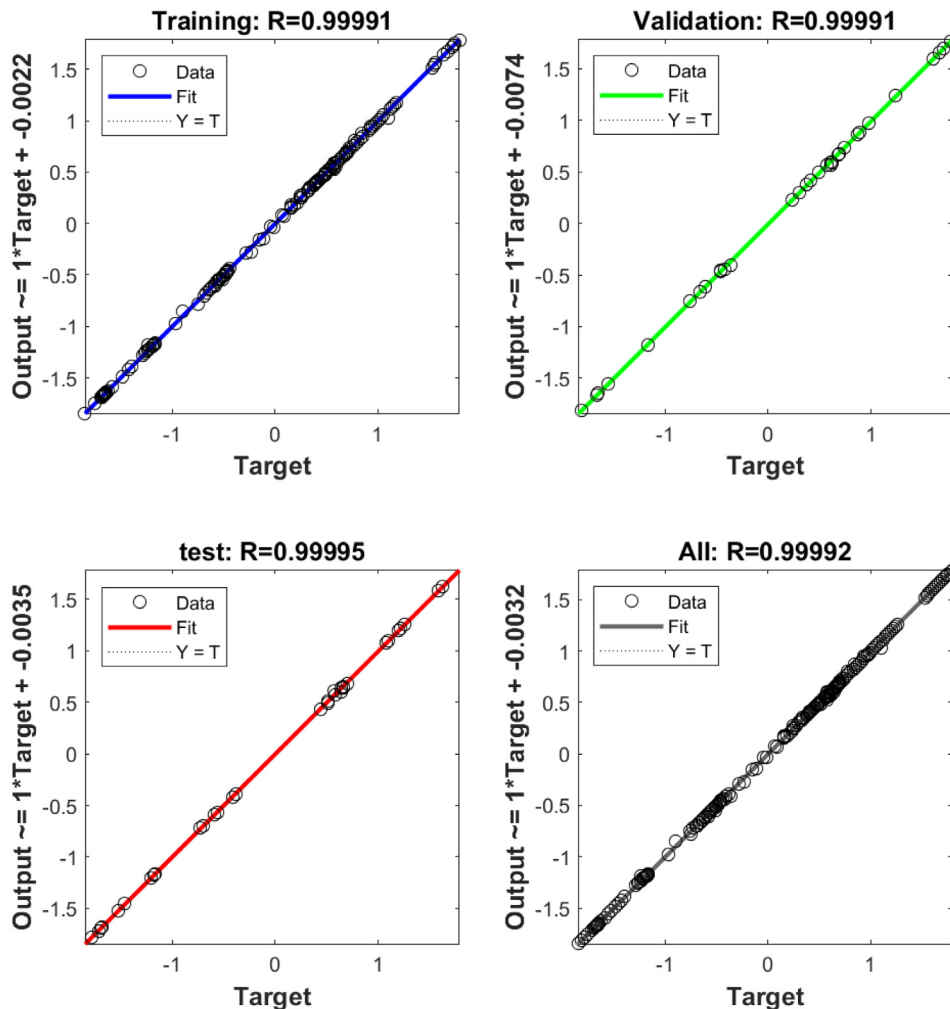


Fig. 6. Correlation plot of the trained ANN.

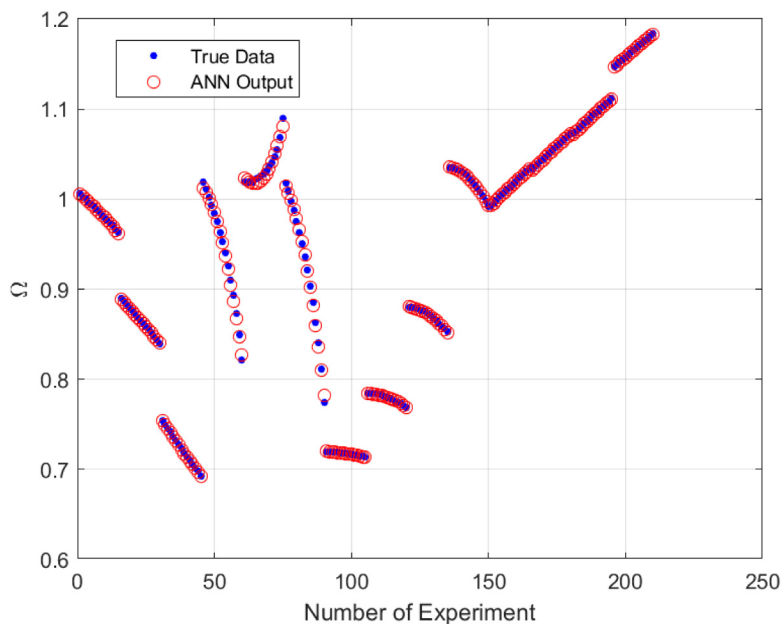


Fig. 7. Comparison of ANN outputs and true data for natural frequency.

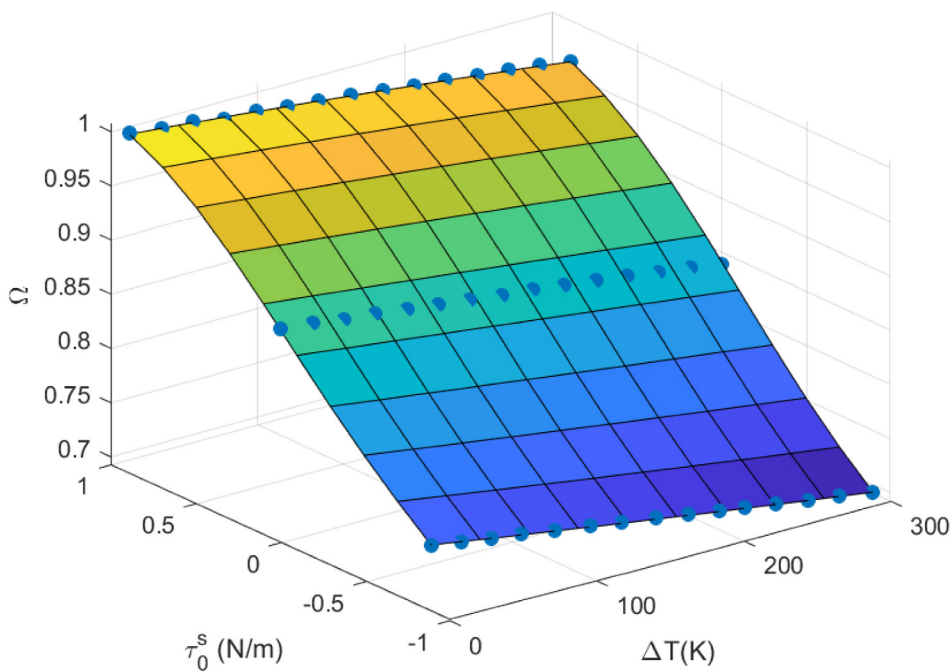


Fig. 8. Natural Frequency versus temperature gradient and residual surface stress.

According to the above figures, several points can be concluded. First of all, the deviation of natural frequency versus temperature gradient is negligible. On the other hand, residual surface stress has a direct and important influence on natural frequency.

Fig. 14 shows that natural frequency has the lowest deviation considering the symmetric distribution pattern of porosity. In contrast, the non-symmetric distribution pattern of porosity results in the highest deviation and effect on natural frequency. Fig. 15 shows that by increasing the porosity parameter, the deviation of natural frequency is monotonically leveled up.

As depicted in Figs. 16–19, we understand the increasing effect of the material length scale parameter on the natural frequency while the nonlocal parameter has almost no effect on the output.

These figures prove the higher effect of shear stiffness on the natural frequency concerning the elastic stiffness of the foundation.

4. Conclusion

In this research, the effect of eight important parameters on the natural frequency of FGP nanobeams rested on elastic medium considering surface effects is investigated and modeled using a Perceptron artificial neural network. Using the obtained ANN, not only one can predict the systems response in various conditions, but also optimization of system can be done using heuristic algorithms in the future works. The trained network is one of the simplest models available having 5 nonlinear neurons in hidden layer and one linear neuron in the output

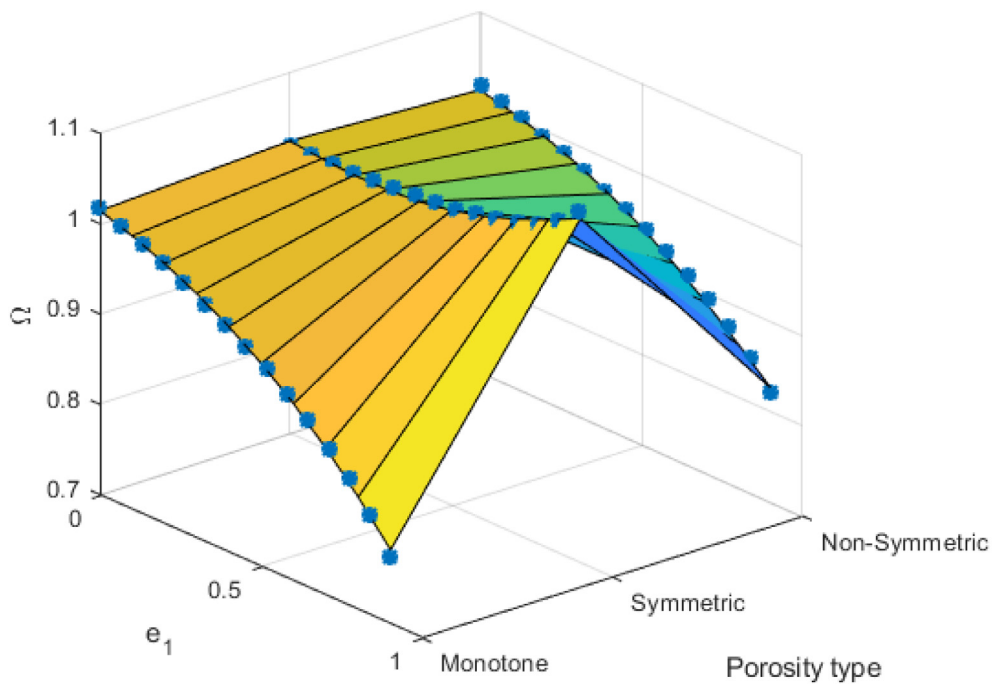


Fig. 9. Natural Frequency versus porosity distribution pattern and porosity parameter.

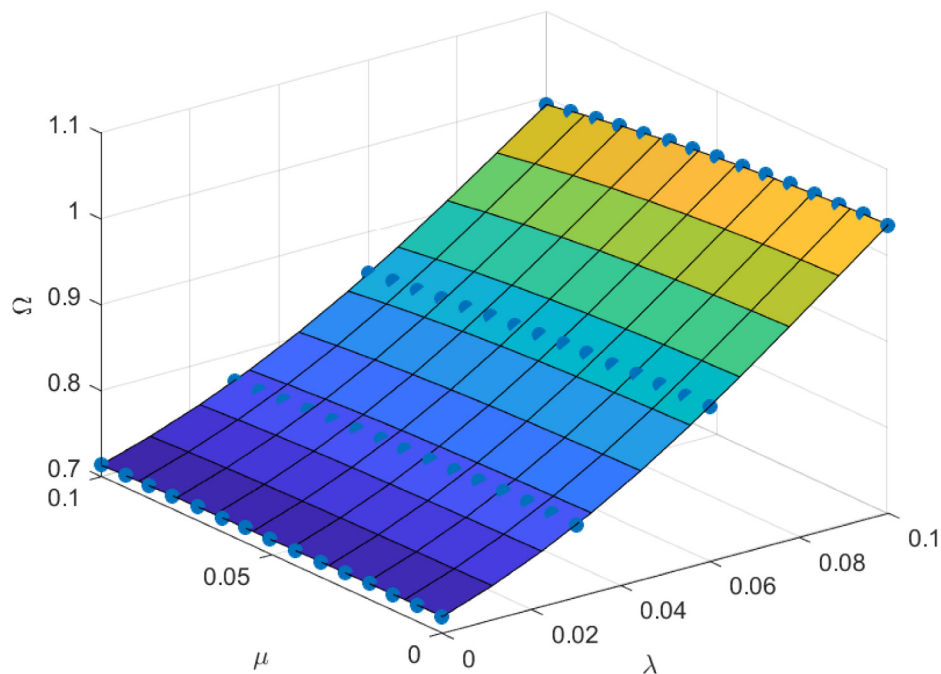


Fig. 10. Natural Frequency versus nonlocal and material length scale parameters.

layer. Due to the fact that obtaining a simplified model to predict the input–output dependency of investigated system is not possible, the obtained model based on ANN can be used for further researches and investigations such as system design or optimization. To this end, an ANN is created and trained using the natural frequency of the system versus eight different parameters. The combination of various levels of these parameters attained 210 different samples for ANN training. The studied parameters are including temperature gradient, residual surface stress, porosity distribution pattern, porosity parameter, nonlocal and material length scale parameters and the elastic and shear stiffness of the Pasternak foundation. Various ANN configurations and training

methods were examined and the optimum network with reasonable performance is chosen by trial and error. Due to the random nature of ANNs, the network is trained 50 times with each training method and the best condition is selected between obtained results. According to obtained performances for training methods, the *trainbr* and *trainlm* have the lowest error. Hence, *trainbr* is selected for further investigations and prediction of natural frequency versus input parameters. After training, the well-trained network is assessed with various indices and graphs. All of the results and graphs prove that the trained network has acceptable performance and could be used for the prediction of natural frequency. Therefore, this network models the system correctly

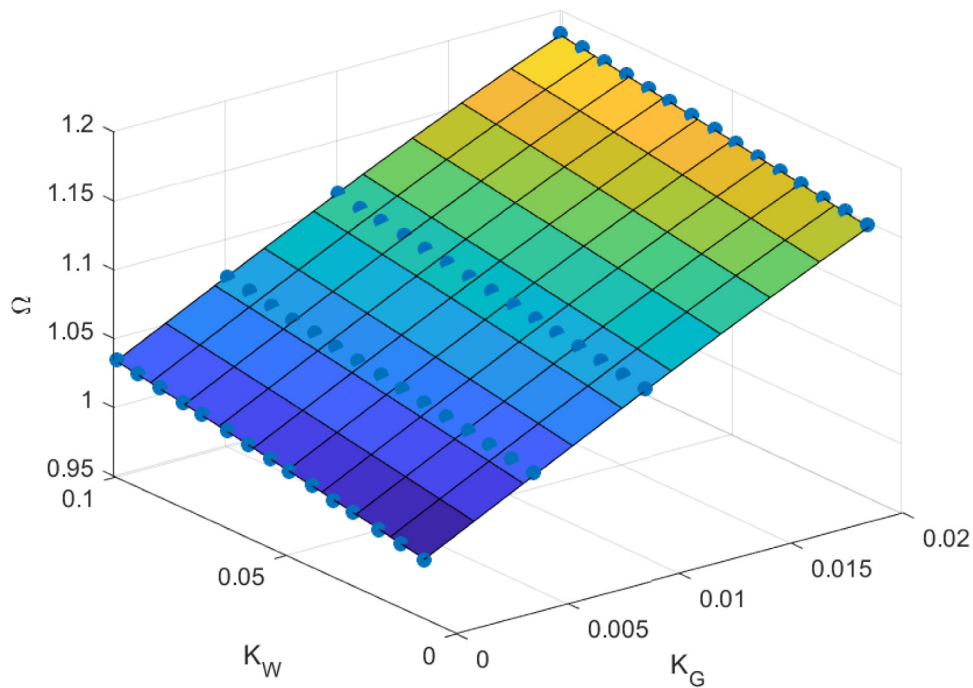


Fig. 11. Natural Frequency versus Pasternak elastic foundation parameters.

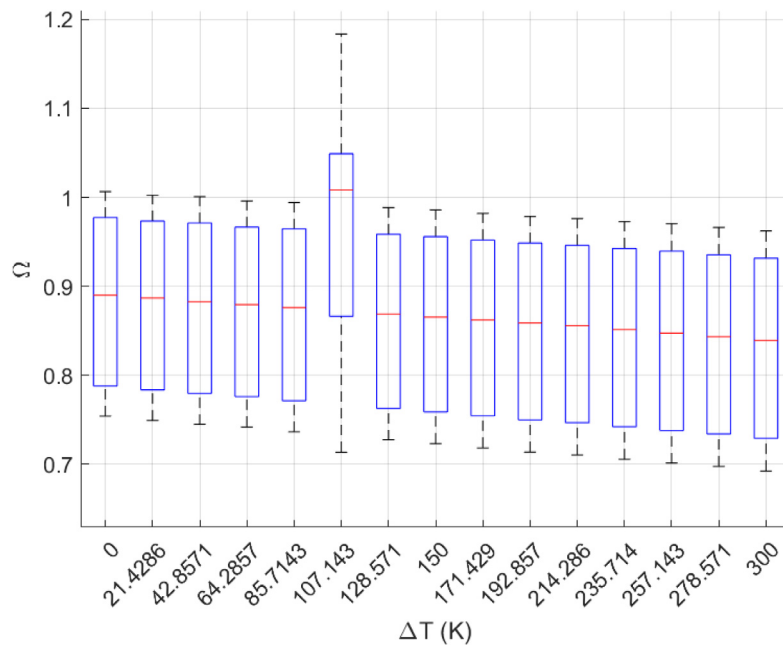


Fig. 12. Natural frequency deviation versus temperature gradient.

Table 6
MSE and performance of various training methods.

Method	trainbfg	trainbr	traincgb	traincgf	traincgp	traingda	traingdx	trainrp	trainscg	trainlm
MSE	4.09E-05	1.37E-07	3.47E-05	6.01E-05	5.11E-05	6.44E-04	2.43E-04	1.00E-04	8.77E-05	3.98E-07

and mimics very well its input-output dependency. Hence, it can be used instead of a long and complicated system of equations for various

reasons including optimization. According to the attained results, the main conclusions can be summarized as follows:

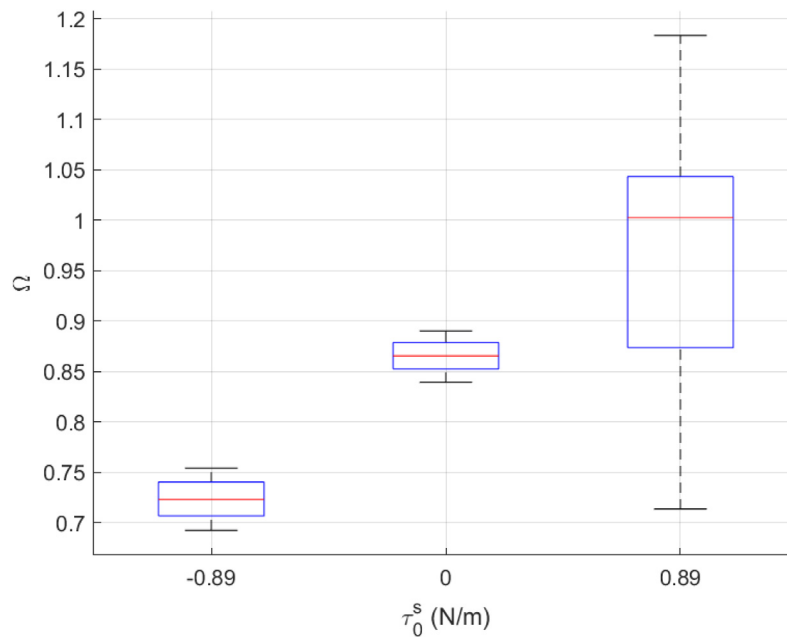


Fig. 13. Natural frequency deviation versus residual surface stress.

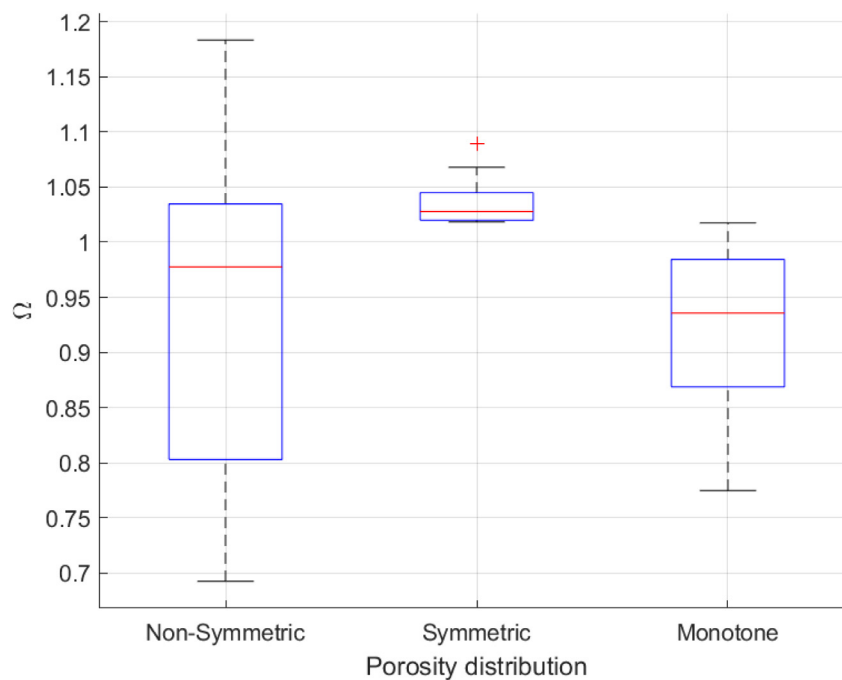


Fig. 14. Natural frequency deviation versus porosity distribution pattern.

- An ANN with 5 nonlinear neurons in the hidden layer and on linear neuron trained well and predicted natural frequency of system accurately.
- Among various training methods for assumed network, *trainbr* and *trainlm* showed to have the highest performance.
- The dependency of the natural frequency is inverse to the temperature gradient and nonlocal parameter in the sense that increasing these factors will decrease the natural frequency. Of course, both of them have a negligible influence on the output in comparison to the rest of the input parameters.
- Increasing the material length scale parameter grows the effect of the nonlocal parameter. In other words, in lower material length scale values, the nonlocal parameter has almost no effect on the output.
- Residual surface stress, material length scale, and Pasternak foundation parameters have a direct effect on the output and among them, the material length scale parameter has a more noticeable effect.
- By increasing the porosity parameter value, the diversity of natural frequency levels up drastically.

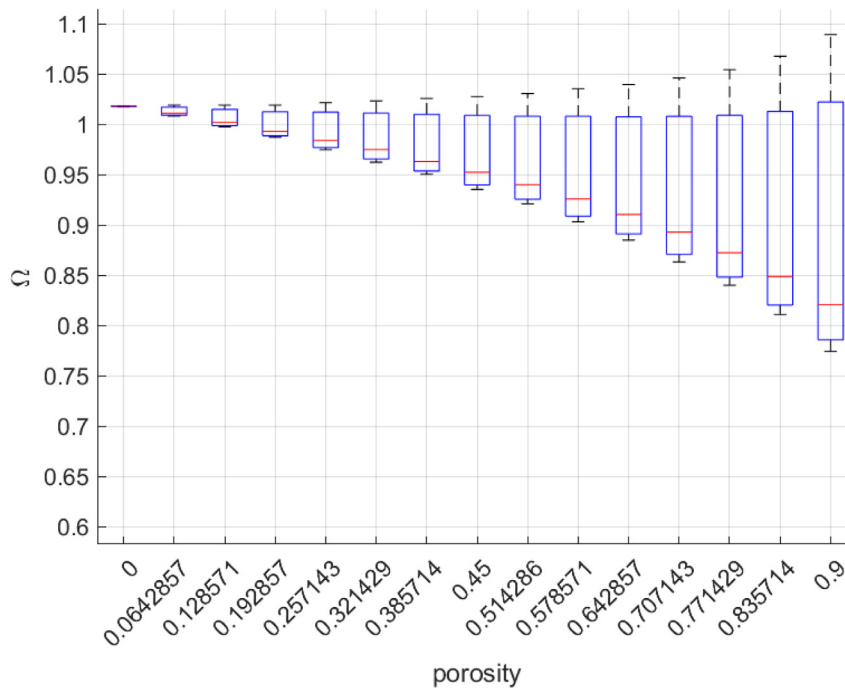


Fig. 15. Natural frequency deviation versus porosity parameter.

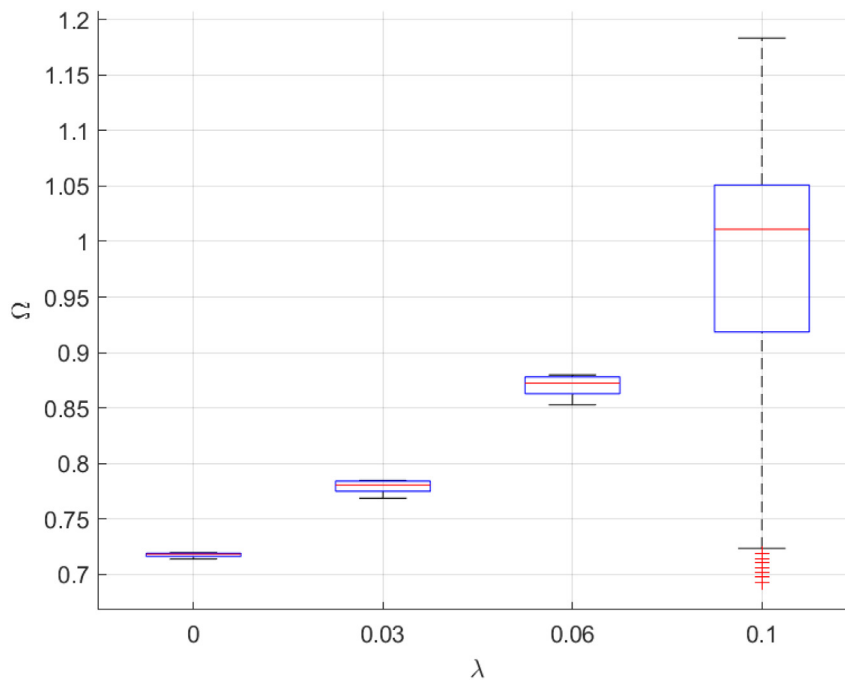


Fig. 16. Natural frequency deviation versus material length scale parameter.

- Among the studied parameters in the investigated margins, the residual surface stress, porosity parameter, shear stiffness and material length scale are the most influential parameters on the natural frequency of nanobeam and have an impressive effect. The rest of the parameters' influence is almost negligible.
- Increasing the porosity parameter in the symmetric porosity distribution pattern increases the natural frequency while in contrast in monotone and nonsymmetric patterns will decrease the frequency with a very high rate.
- Tensional residual stresses cause higher values of natural frequency in contrast to compressional residual stresses.

The obtained results and parameter effects can be used for the design and optimization of micro and nanoscale systems based on porous nanobeams resting in elastic media and considering material and non-local scale parameters.

CRedit authorship contribution statement

Xiaofei Cheng: Methodology, Software, Validation, Writing – original draft, Investigation. **Sara Hakem Al-Khafaji:** Writing – original draft, Investigation. **Mohammad Hashemian:** Writing – original draft,

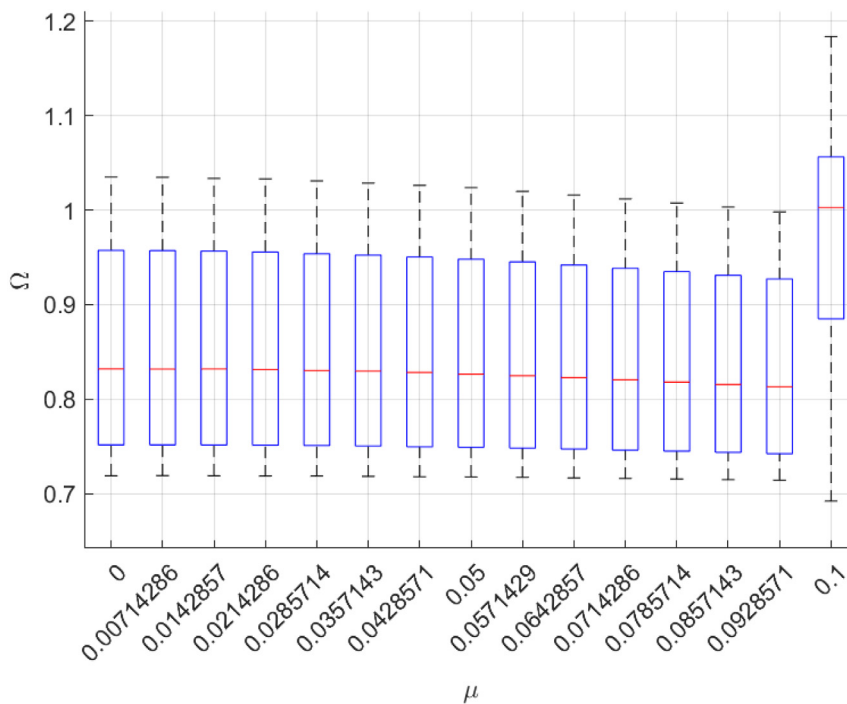


Fig. 17. Natural frequency deviation versus nonlocal parameter.

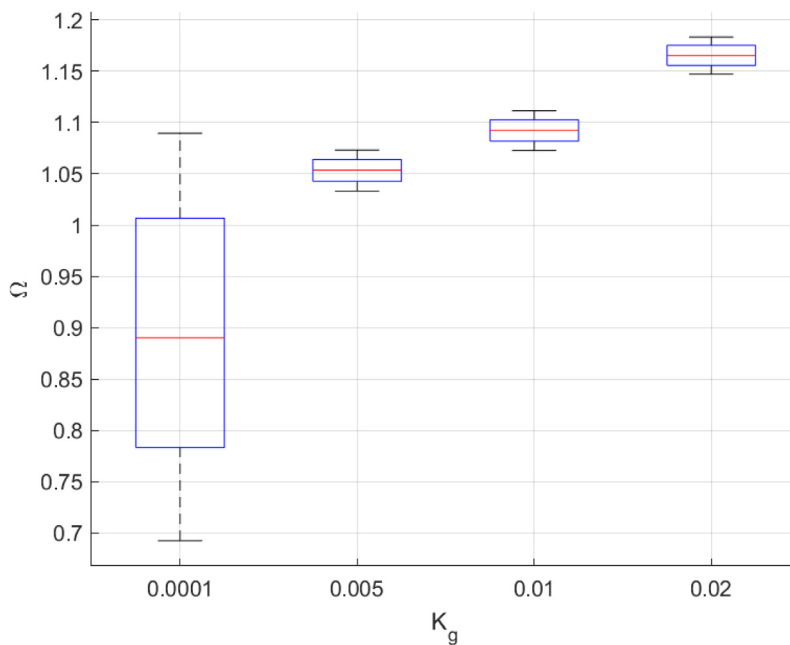


Fig. 18. Natural frequency deviation versus shear stiffness of Pasternak foundation.

Investigation. **Mariem Ahmed:** Writing – original draft, Investigation. **S. Ali Eftekhari:** Methodology, Software, Validation, Writing – original draft, Revision. **Ali Ihsan Alanssari:** Methodology, Software, Validation, Revision. **Nabaa Muhammad diaa:** Methodology, Software, Validation, Writing – original draft, Revision. **Manal Morad Karim:** Methodology, Software, Validation, Writing – original draft. **Davood Toghraie:** Methodology, Software, Validation, Writing – original draft, Revision. **Ahmed Hussien Alawadi:** Methodology, Software, Validation, Revision.

Declaration of competing interest

The authors declare that they have no known competing financial interests or personal relationships that could have appeared to influence the work reported in this paper.

Data availability

No data was used for the research described in the article.

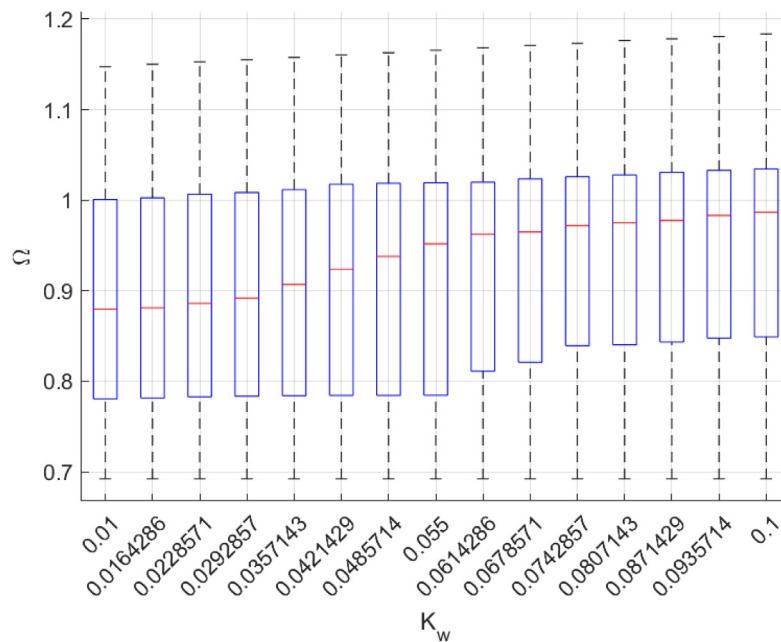


Fig. 19. Natural frequency deviation versus elastic stiffness of Pasternak foundation.

References

- Ahmad, F., 2022. Deep image retrieval using artificial neural network interpolation and indexing based on similarity measurement. *CAAI Trans. Intell. Technol.* 7 (2), 200–218. <http://dx.doi.org/10.1049/cit2.12083>.
- Al Rjoub, Y.S., Alshatnawi, J.A., 2020. Free vibration of functionally-graded porous cracked plates. *Structures* 28, 2392–2403.
- Anon, 1995. *Artificial Neural Networks, An Introduction to ANN Theory and Practice*, first ed. Springer, Berlin, Heidelberg.
- Aria, A.I., Rabczuk, T., Friswell, M.I., 2019. A finite element model for the thermoelastic analysis of functionally graded porous nanobeams. *Eur. J. Mech. - A/Solids* 77, 103767.
- Babaei, H., Eslami, M.R., 2021. On nonlinear vibration and snap-through buckling of long FG porous cylindrical panels using nonlocal strain gradient theory. *Compos. Struct.* 256, 113125.
- Barati, M.R., 2017. Investigating dynamic response of porous inhomogeneous nanobeams on hybrid Kerr foundation under hygro-thermal loading. *Appl. Phys. A* 123, 332.
- Chen, Z., 2022. Research on internet security situation awareness prediction technology based on improved RBF neural network algorithm. *J. Comput. Cognitive Eng.* 1 (3), 103–108. <http://dx.doi.org/10.47852/bonviewJCCE149145205514>.
- Chen, D., Kitipornchai, S., Yang, J., 2016. Nonlinear free vibration of shear deformable sandwich beam with a functionally graded porous core. *Thin-Walled Struct.* 107, 39–48.
- Chen, W., Wang, L., Dai, H., 2019a. Nonlinear free vibration of nanobeams based on nonlocal strain gradient theory with the consideration of thickness-dependent size effect. *J. Mech. Mater. Struct.* 14, 119–137.
- Chen, W., Wang, L., Dai, H., 2019b. Stability and nonlinear vibration analysis of an axially loaded nanobeam based on nonlocal strain gradient theory. *Int. J. Appl. Mech.* 11, 1950069.
- Chen, D., Yang, J., Kitipornchai, S., 2015. Elastic buckling and static bending of shear deformable functionally graded porous beam. *Compos. Struct.* 133, 54–61.
- Deng, C., Zhang, L., Deng, H., 2022. Improving sentence simplification model with ordered neurons network. *CAAI Trans. Intell. Technol.* 7 (2), 268–277. <http://dx.doi.org/10.1049/cit2.12047>.
- Dey, S., Mukhopadhyay, T., Spickenheuer, A., Gohs, U., Adhikari, S., 2016. Uncertainty quantification in natural frequency of composite plates - An artificial neural network based approach. *Adv. Compos. Lett.* 25, 096369351602500203.
- Eltaher, M.A., Mahmoud, F.F., Assie, A.E., Meletis, E.I., 2013. Coupling effects of nonlocal and surface energy on vibration analysis of nanobeams. *Appl. Math. Comput.* 224, 760–774.
- Enayat, S., Hashemian, M., Toghraie, D., Jaberzadeh, E., 2020a. A comprehensive study for mechanical behavior of functionally graded porous nanobeams resting on elastic foundation. *J. Braz. Soc. Mech. Sci. Eng.* 42, 420.
- Enayat, S., Hashemian, M., Toghraie, D., Jaberzadeh, E., 2020b. Bending, buckling and vibration analyses of FG porous nanobeams resting on Pasternak foundation incorporating surface effects. *ZAMM - J. Appl. Math. Mech./ Z. Angew. Math. Und Mech.* e202000231.
- Eringen, A.C., 1983. On differential equations of nonlocal elasticity and solutions of screw dislocation and surface waves 54. pp. 4703–4710.
- Fan, G., A.S E-S, Eftekhari, S.A., Hekmatifar, M., Toghraie, D., Mohammed, A.S., et al., 2022. A well-trained artificial neural network (ANN) using the trainlm algorithm for predicting the rheological behavior of water – ethylene glycol/WO3 – MWCNTs nanofluid. *Int. Commun. Heat Mass Transf.* 131, 105857.
- Fleck, N.A., Hutchinson, J.W., 2001. A reformulation of strain gradient plasticity. *J. Mech. Phys. Solids* 49, 2245–2271.
- Foroutan, S., Hashemian, M., Khandan, A., 2020. A novel porous graphene Scaffold prepared using freeze-drying technique for orthopedic approaches: Fabrication and buckling simulation using GDQ method. *IUST* 17, 62–76.
- Foroutan, S., Hashemian, M., Khosravi, M., Nejad, M.G., Asefnejad, A., Saber-Samandari, S., et al., 2021. A porous sodium alginate-CaSiO₃ polymer reinforced with graphene nanosheet: Fabrication and optimality analysis. *Fibers Polym.* 22, 540–549.
- Garg, A., Belarbi, M.-O., Tounsi, A., Li, L., Singh, A., Mukhopadhyay, T., 2022. Predicting elemental stiffness matrix of FG nanoplates using Gaussian process regression based surrogate model in framework of layerwise model. *Eng. Anal. Bound. Elem.* 143, 779–795.
- Gong, J., Xuan, L., Ying, B., Wang, H., 2019. Thermoelastic analysis of functionally graded porous materials with temperature-dependent properties by a staggered finite volume method. *Compos. Struct.* 224, 111071.
- Gurtin, M.E., Ian Murdoch, A., 1978. Surface stress in solids. *Int. J. Solids Struct.* 14, 431–440.
- Gurtin, M.E., Murdoch, A.I., 1975. A continuum theory of elastic material surface. *Arch. Ration. Mech. Anal.* 57, 291–323.
- Hanif, R., Mustafa, S., Iqbal, S., Piracha, S., 2022. A study of time series forecasting enrollments using fuzzy interval partitioning method. *J. Comput. Cognitive Eng.* <http://dx.doi.org/10.47852/bonviewJCCE2202159>.
- Hashemzadeh, H., Eftekhari, S., Loh-Mousavi, M., 2017. Forging pre-form dies optimization using artificial neural networks and continuous genetic algorithm.
- Kao, C.Y., Hung, S.-L., 2003. Detection of structural damage via free vibration responses generated by approximating artificial neural networks. *Comput. Struct.* 81, 2631–2644.
- Khan, J., Lee, E., Kim, K., 2022. A higher prediction accuracy-based alpha-beta filter algorithm using the feedforward artificial neural network. *CAAI Trans. Intell. Technol.* 1-16, <http://dx.doi.org/10.1049/cit2.12148>.
- Kumar, R.R., Mukhopadhyay, T., Pandey, K.M., Dey, S., 2019. Stochastic buckling analysis of sandwich plates: The importance of higher order modes. *Int. J. Mech. Sci.* 152, 630–643.
- Lam, D.C.C., Yang, F., Chong, A.C.M., Wang, J., Tong, P., 2003. Experiments and theory in strain gradient elasticity. *J. Mech. Phys. Solids* 51, 1477–1508.
- Li, L., Tang, H., Hu, Y., 2018. The effect of thickness on the mechanics of nanobeams. *Int. J. Eng. Sci.* 123, 81–91.
- Lim, C.W., Zhang, G., Reddy, J.N., 2015. A higher-order nonlocal elasticity and strain gradient theory and its applications in wave propagation. *J. Mech. Phys. Solids* 78, 298–313.
- Lu, L., Guo, X., Zhao, J., 2019. A unified size-dependent plate model based on nonlocal strain gradient theory including surface effects. *Appl. Math. Model.* 68, 583–602.

- Maurya, M., Sadarang, J., Panigrahi, I., Dash, D., 2021. Detection of delamination in carbon fibre reinforced composite using vibration analysis and artificial neural network. *Mater. Today: Proc.*
- Mindlin, R.D., 1965. Second gradient of strain and surface-tension in linear elasticity. *Int. J. Solids Struct.* 1, 417–438.
- Moshayedi, A.J., Roy, A.S., Kolahdooz, A., Shuxin, Y., 2022. Deep learning application pros and cons over algorithm. *EAI Endorsed Trans. AI Robot.* 1, 1–13.
- Naeimi, A., Loh Mousavi, M., Eftekhari, A., 2014. Optimum designing of forging preform die for the H-shaped parts using backward deformation method and neural networks algorithm. *J. Mod. Processes Manuf. Prod.* 3, 79–96.
- Rafieian, S., Hashemian, M., Pirmoradian, M., 2017. Buckling analysis of double-layer piezoelectric nanoplates surrounded by elastic foundations and thermal environments considering nonlocal and surface energy models. *J. Mech.* 34, 483–494.
- Sharma, S., Verma, K., Hardaha, P., 2022. Implementation of artificial intelligence in agriculture. *J. Comput. Cognitive Eng.* <http://dx.doi.org/10.47852/bonviewJCCE2202174>.
- She, G.-L., Yuan, F.-G., Ren, Y.-R., Liu, H.-B., Xiao, W.-S., 2018. Nonlinear bending and vibration analysis of functionally graded porous tubes via a nonlocal strain gradient theory. *Compos. Struct.* 203, 614–623.
- Tang, H., Li, L., Hu, Y., 2019a. Coupling effect of thickness and shear deformation on size-dependent bending of micro/nano-scale porous beams. *Appl. Math. Model.* 66, 527–547.
- Tang, H., Li, L., Hu, Y., Meng, W., Duan, K., 2019b. Vibration of nonlocal strain gradient beams incorporating Poisson's ratio and thickness effects. *Thin-Walled Struct.* 137, 377–391.
- Truong, T.T., Lee, S., Lee, J., 2020. An artificial neural network-differential evolution approach for optimization of bidirectional functionally graded beams. *Compos. Struct.* 233, 111517.
- Xia, J.S., Khaje Khabaz, M., Patra, I., Khalid, I., Alvarez, J.R.N., Rahmanian, A., et al., 2022. Using feed-forward perceptron artificial neural network (ANN) model to determine the rolling force, power and slip of the tandem cold rolling. *ISA Trans.*
- Xiang, Y., Jiang, H., Lu, J., 2017. Analyses of dynamic characteristics of a fluid-filled thin rectangular porous plate with various boundary conditions. *Acta Mech. Solida Sin.* 30, 87–97.
- Xie, X., Xie, M., Moshayedi, A.J., Noori Skandari, M.H., 2022. A hybrid improved neural networks algorithm based on L2 and dropout regularization. *Math. Probl. Eng.* 2022, 8220453.
- Yang, F., Chong, A.C.M., Lam, D.C.C., Tong, P., 2002. Couple stress based strain gradient theory for elasticity. *Int. J. Solids Struct.* 39, 2731–2743.
- Yildirim, S., 2021. Free vibration of axially or transversely graded beams using finite-element and artificial intelligence. *Alex. Eng. J.*
- Yin, Z., Gao, H., Lin, G., 2021. Bending and free vibration analysis of functionally graded plates made of porous materials according to a novel the semi-analytical method. *Eng. Anal. Bound. Elem.* 133, 185–199.